Charge-Transfer Band Splittings in Electronic Spectra of Mixed Ligand Halogeno Osmium(IV) Complexes

Hans-Herbert Schmidtke* and Nicolai Lehnert

Institut für Theoretische Chemie, Heinrich-Heine-Universität Düsseldorf, D-40225 Düsseldorf, Germany

Received February 13, 1998

The charge-transfer absorption spectra of $Cs_2[OsCl_5Br]$, $Cs_2[OsCl_4Br_2]$ (cis) and (trans), $Cs_2[OsBr_5Cl]$, and $Cs_2[OsBr_4Cl_2]$ (cis) are measured from microcrystals in KBr disks at 2 K and compared to corresponding $Cs_2[OsCl_6]$ and $Cs_2[OsBr_6]$ spectra recorded with the same technique. The observed band shifts and band splittings due to lower molecular symmetry are interpreted using perturbation methods on the basis of molecular orbital theory which considers interligand orbital interactions as most important. For complexes containing more bromide than chloride ligands, spin−orbit coupling on the ligands must be included. Since coupling conditions are close to the j−j coupling limit band assignments to orbital transitions are obtained. The spectra in the region up to 33 000 cm^{-1} are explained by ligand to metal charge-transfer transitions starting from metal−ligand π-bonded orbitals t_{1g}, t_{1u}, and t_{2u} (and t_{2g}). Corresponding σ orbitals and intermixing with metal−ligand π orbitals could be neglected due to energy reasons. Band splittings and assignments to irreducible representations of low symmetry point groups are obtained from parameter relations. Due to the large number of orbital interaction parameters which exceeds the number of electronic transitions observable, numerical eigenvalue calculations from pertubation matrixes have not been carried out.

1. Introduction

The assignment of d−d transitions in complex spectra of transition group ions for evaluating electronic structures is conveniently obtained by applying ligand field theory or angular overlap model (AOM) calculations. Reliable interpretations of charge transfer bands on the basis of theoretical models have been achieved only for octahedral coordination. Since the pioneering work of Jørgensen,[1] who started investigating solution spectra of hexahalogeno complexes of heavy transition group ions, more detailed measurements were carried out on charge-transfer spectra of ions doped in crystals which supply exact octahedral fields. For Os(IV), absorption spectra at liquid helium temperature have been reported using various cubic host crystals as Cs_2ZrCl_6 and Cs_2ZrBr_6.[2−4] Diffuse reflectance spectra of pure compounds are poorly resolved and have not been assigned to symmetry species.[5] Low-symmetry spectra have been interpreted by Jørgensen and Preetz[6,7] who considered solution spectra of tetragonal mixed halide complexes. More detailed spectra at low temperature are reported only on trans-mixed hexahalogeno complexes of tetrabutylammonium salts pressed in KBr pellets.[8] Mixed ligand complexes with amine and halogen ligands show charge-transfer bands due to electron transfer from the halogen with no contributions from amine ligand orbitals. They can be explained by a qualitative MO model on the basis of symmetry considerations.[9,10] The latter work neglects, however, the inclusion of interligand orbital interactions which essentially contribute to the explanation of MCD spectra of $IrCl_6^{2-}$ [6,11] and $OsCl_6^{2-}$.[3]

In the present work we report absorption spectra of some tetragonal (C_{4v}, D_{4h} point symmetry) and cis-disubstituted (C_{2v}) mixed halogeno complexes of Os(IV) which became available more recently. The spectra recorded at low temperature (2 K) show more details and have in general peak positions different from those in solution;[6,7,12] they are of comparable quality to the solid-state spectra of the trans-mixed halogeno complexes[8] but do not obtain the resolution of doped materials.[3,4]

The assignment of low-symmetry charge-transfer bands will be carried out using ligand orbital energies which are calculated in terms of orbital parameters similar to those used in the angular overlap model (AOM). In particular, the interactions between orbitals of (nonbonded) ligands are included which supply important contributions to the energy levels of ligand molecular orbitals (MO).[3,6,8,11] For compounds with a majority of bromide ligands, spin−orbit coupling on this ligand must be also considered due to the large effect on the band splittings. The perturbation matrixes calculated from these interactions supply nondiagonal elements which contribute significantly to the low-symmetry splittings of octahedral energy levels. Due to many combinations of levels of equal symmetry in the case of double groups, the calculation of the spin−orbit coupling matrixes is more elaborate.

Because of the large number of parameters simulating the various types of metal−ligand and ligand−ligand interactions which exceeds the number of experimentally available peak

(1) Jørgensen, C. K. *Mol. Phys.* **1959**, *2*, 309.
(2) Dorain, P. B.; Patterson, H. H.; Jordan, P. C. *J. Chem. Phys.* **1968**, *49*, 3845.
(3) Piepho, S. B.; Dickinson, J. R.; Spencer, J. A.; Schatz, P. N. *Mol. Phys.* **1972**, *24*, 609.
(4) Inskeep, W. H.; Schwartz, R. W.; Schatz, P. N. *Mol. Phys.* **1973**, *25*, 805.
(5) Allen, G. C.; Al-Mobarak, R.; El-Sharkawy, G. A. M.; Warren, K. D. *Inorg. Chem.* **1972**, *11*, 787.
(6) Jørgensen, C. K.; Preetz, W. *Z. Naturforsch.* **1967**, *22A*, 945.
(7) Preetz, W. *Z. Anorg. Allg. Chem.* **1966**, *348*, 151.
(8) Piepho, S. B.; Inskeep, W. H.; Schatz, P. N.; Preetz, W.; Homborg, H. *Mol. Phys.* **1975**, *30*, 1569.
(9) Verdonck, E.; Vanquickenborne, L. G. *Inorg. Chem.* **1974**, *13*, 762.
(10) Lever, A. B. P. *Inorganic Electronic Spectroscopy*, 2nd ed.; Elsevier: Amsterdam, 1984.
(11) Henning, G. N.; McCaffery, A. J.; Schatz, P. N.; Stephens, P. J. *J. Chem. Phys.* **1968**, *48*, 5656.
(12) Kennedy, B. J.; Heath, G. A. *Inorg. Chim. Acta* **1992**, *195*, 101.

10.1021/ic980168+ CCC: $15.00
Published on Web 11/13/1998

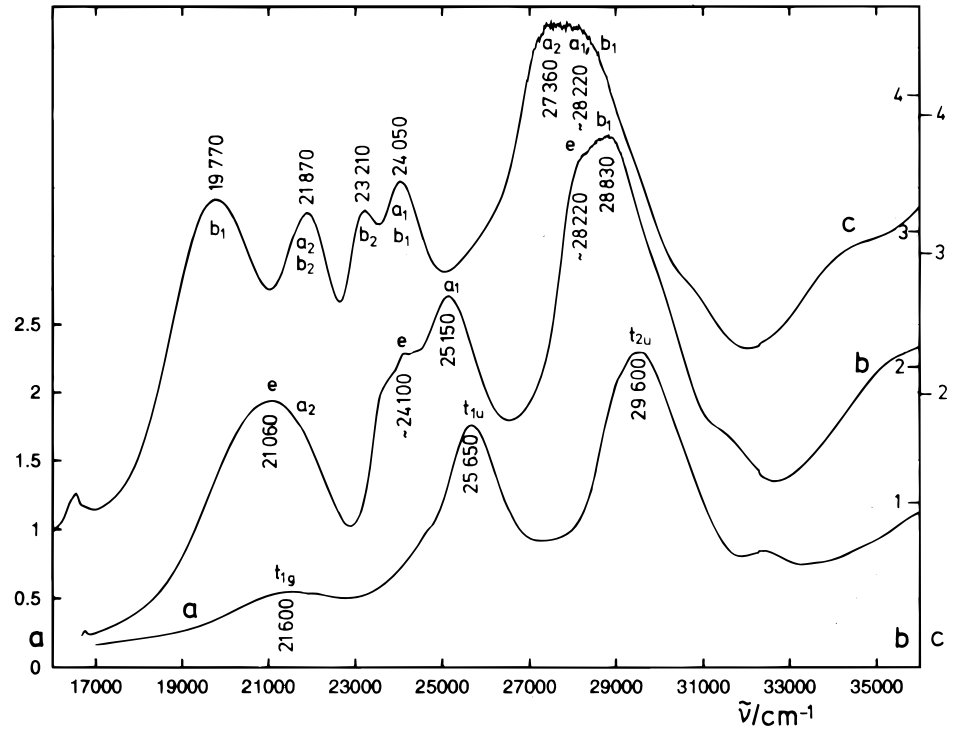

Figure 1. Absorption spectra of $Cs_2[OsCl_6]$ (a), $Cs_2[OsCl_5Br]$ (b), and $Cs_2[OsCl_4Br_2]$ (cis) (c) recorded at 2 K from microcrystals in KBr disks. Intensities are in arbitrary units at different scales, as indicated.

positions, a fitting procedure to theoretical energy expressions is not possible. Rather, we apply the present MO model for obtaining band assignments, band shifts, and level splittings by the use of well-known relations of parameter values describing σ- and π-bonding energies and spin−orbit coupling constants of chloride and bromide ligands.

2. Experimental Section

The compounds have been prepared and purified using the procedures given in refs 6, 7, 13, and 14 and references therein.

The optical spectra were recorded on a Cary 4E instrument containing a tungsten lamp as light source, a 25 cm double monochromator, and a photomultiplier with an S20 photocathode as detector. The spectra are recorded from powdered microcrystals pressed in KBr disks (concentrations of about 1 mg of complex compound in 600 mg KBr) immediately before use. Possible solid-state reactions with KBr were controlled by repeated recording of the spectra.

The samples were cooled by immersion into superfluid helium using a Konti bathcryostat type Spectro C of CryoVac. The cooling capacity guarantees temperatures slightly below 2 K on the samples when exposed to radiation. The absorption spectra measured are illustrated in Figure 1−4. Spectra of complexes mainly containing chloride or bromide ligands are displayed on separate plots in order to demonstrate band shifts and band splittings due to subsequent ligand substitution. They differ in many respects from those reported in solution.[6,7,12]

3. Theoretical

3.1. The Model. The charge-transfer spectra of Os(IV) halogeno complexes are largely determined by ligand-to-metal orbital transitions. Electron repulsion is of minor importance. This follows from the close similarity of Ir(IV) and Os(IV) hexahalogeno spectra which show equal band structures due respectively to $\gamma_i^6 t_{2g}^5 \rightarrow \gamma_i^5 t_{2g}^6$ and $\gamma_i^6 t_{2g}^4 \rightarrow \gamma_i^5 t_{2g}^5$ electron transitions in the j−j coupling limit (γ_i ligand orbitals t_{1g}, t_{1u}, t_{2u}, etc. and t_{2g} even ligand field d-orbital component of central metals).[1−3,8] Multiplets arising from a given orbital configurations are therefore closely degenerate. This obviously holds for mixed-ligand complexes as well.[6,8] Indeed, a molecular orbital analysis supplies, when spin−orbit coupling is neglected, only two parity-allowed one-electron transitions from π-bonded ligand orbitals which correspond to $t_{1u} \rightarrow t_{2g}$ and $t_{2u} \rightarrow t_{2g}$ transitions in octahedral Os(IV) and Ir(IV) complexes.[3,11] For large spin−orbit coupling the first orbital transition corresponds to e'_u, $u'_u \rightarrow e''_g$ (O_h* double group notation as in ref 3 which equals to $e' = e_{1/2}$, $e'' = e_{5/2}$, and $u' = g_{3/2}$ in other text books[15]) and the second to e''_u, $u'_u \rightarrow e''_g$ yielding four transitions, three of them ($e'_u \rightarrow e''_g$ is not allowed) being clearly identified in Os(IV) and in Ir(IV) hexabromo spectra.[1,4,16] For a survey see the orbital diagrams in Figure 5.

The present procedure therefore considers a common molecular orbital model which was also used for earlier interpretations of charge-transfer spectra of octahedral MX_6 complexes.[3−5,11,12,16−18] This assumes an electronic structure of charge transfer states which is well represented by wave functions resulting from $(t_{2g})^{n+1} \times (\gamma_i)^5$ electron configurations where t_{2g} is a d-orbital and $\gamma_i = t_{1g}$, t_{1u}, t_{2u}, ... are ligand orbitals of appropriate symmetry. Ligand-to-metal charge transfer is therefore described by electron transfer from γ_i orbitals to one of the t_{2g} central metal orbitals. The model has been applied as well in cases of lower symmetry.[6,8−10]

Due to the importance of ligand−ligand orbital interaction, which became obvious from the interpretation of MCD spec-

(13) Strand, D.; Linder, R.; Schmidtke, H.-H. *Mol. Phys.* **1990**, *71*, 1075.
(14) Schmidtke, H.-H.; Lehnert, N.; Giesbers, M. *Spectrochim. Acta* **1997**, *53A*, 789.
(15) Flurry, R. L. *Symmetry Groups*; Prentice Hall: Englewood Cliffs, NJ, 1980.
(16) Dickinson, J. R.; Piepho, S. B.; Spencer, J. A.; Schatz, P. N. *J. Chem. Phys.* **1972**, *56*, 2668.

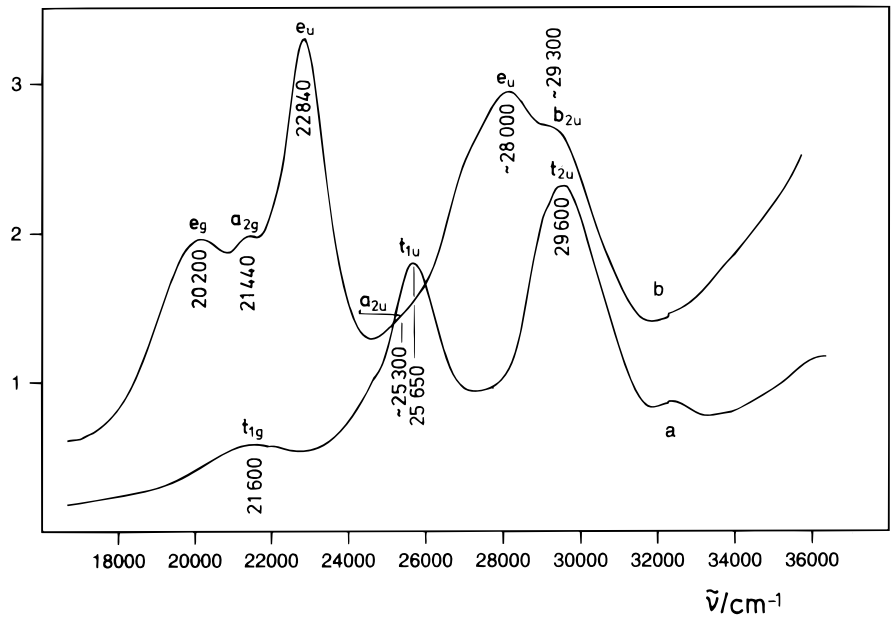

Figure 2. Absorption spectra of $Cs_2[OsCl_6]$ (a) and $Cs_2[OsCl_4Br_2]$ (trans) (b) recorded and illustrated as described in Figure 1.

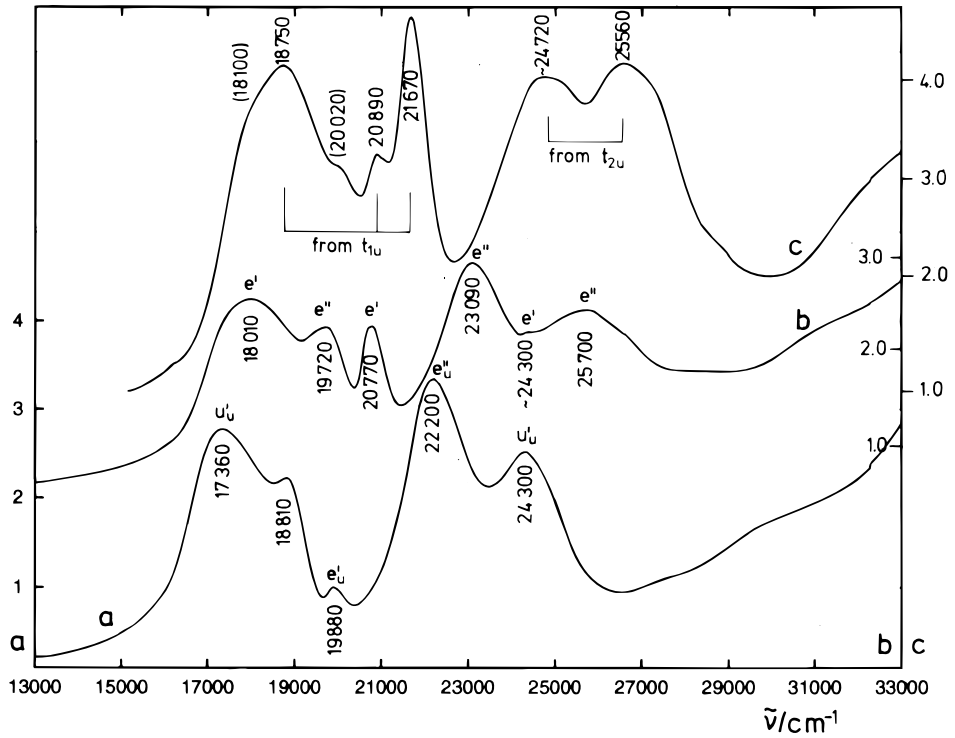

Figure 3. Absorption spectra of $Cs_2[OsBr_6]$ (a), $Cs_2[OsBr_5Cl]$ (b), and $Cs_2[OsBr_4Cl_2]$ (cis) (c) recorded and illustrated as described in Figure 1.

tra,[3,4,8,11,16,17] this interaction is considered with priority for estimating the ligand orbital energies γ_i. The spin−orbit coupling is of equal importance in the case where the complex contains more of the heavier ligands (bromide, iodide). Metal−ligand orbital interaction $t_{2g}-p_\pi$ is identical for all ligands and enters on ligand substitution X by Y in MX_6 only by parameter changes or parameter relations.

3.2. Model Parameters. The interligand interaction parameters are σ and π for X−X p_σ and p_π orbital pairs at maximal overlap position, σ' and π' for X−Y and σ'',π'' for Y−Y ligand pairs. These parameters are negative due to the energy gain for bonding; negative signs indicate antibonding interactions. Nondiagonal elements and level shifts due to the ligand substitution of X by Y can be written in terms of bond changes $\Delta\sigma = \sigma - \sigma'$, $\Delta\pi = \pi - \pi'$, $\Delta'\sigma = \sigma - \sigma''$ and $\Delta'\pi = \pi - \pi''$ which are negative if the substitute Y is a heavier halogen (e.g., Br) than X (Cl), because we have $\sigma < \sigma'$, $\pi < \pi'$ and $\sigma' < \sigma''$ and $\pi' < \pi''$. Reverse substitution requires change of signs. In addition, a further parameter ΔE considers the energy change of p orbitals on the halogens X and Y which for free ions corresponds to the difference in ionization energies, with ΔE positive for X = Cl and Y = Br and negative for reverse substitution.

For an octahedral MX_6 (O_h) complex the ligand molecular orbitals forming π bonds $M-L^\pi$ to the central metal, the following sequence of decreasing energies is obtained:

$$t_{1g}(-\sigma - \pi) > t_{1u}(2\pi) > t_{2u}(-2\pi) > t_{2g}(\sigma + \pi) \quad (1)$$

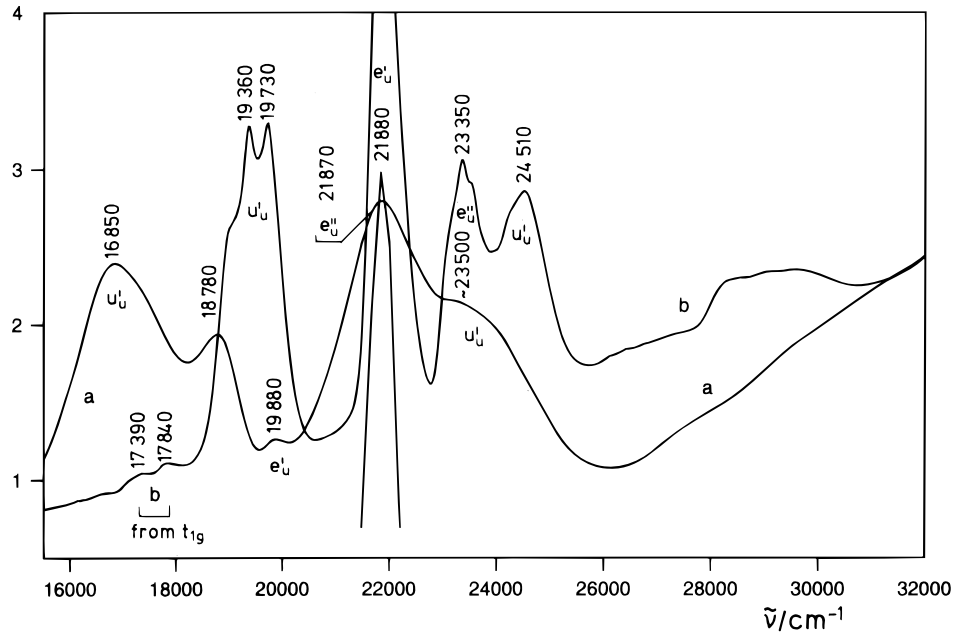

Figure 4. Absorption spectra of $K_2[OsBr_6]$ (a) and $(Bu_4N)_2[OsBr_6]$ (b) recorded and illustrated as described in Figure 1.

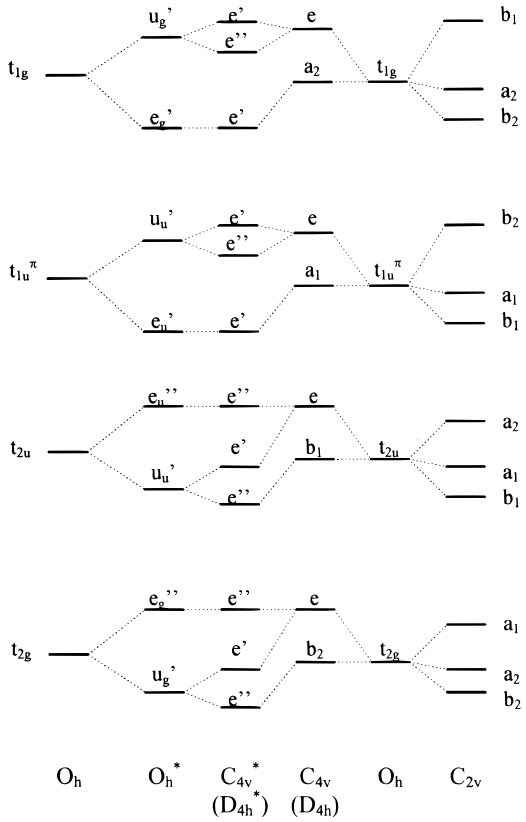

Figure 5. Orbital energy diagrams (schematic) indicating possible splitting assignments for various symmetries. Starred group symbols refer to double (spinor) groups. Orbital transitions into the lowest d-orbital component of Os(IV) forbidden by electric dipole radiations are marked by (−), all others are allowed. For C_{2v} symmetry, transitions from a_2 into higher t_{2g} d orbital components are allowed.

The AOM orbital energies which result from considering only inter-halogen σ and π interactions (with energy parameters $\sigma < \pi$) are given in brackets. The energy expressions are calculated from corresponding symmetry orbitals which for O_h are, e.g., in refs 6 and 8. The sequence in eq 1 follows the AOM ligand orbital energies, except for t_{1u} which is further destabilized due to combinations with lower lying $t_{1u}\sigma$ orbitals forming σ bonds $M-L^{\sigma}$ with the metal. In the case of strong spin−orbit coupling the orbitals assume spin−orbital character $\gamma_i \times e'$.

For heavier halogens spin−orbit coupling on the ligands is included by calculating spin−orbit pertubation matrices with the operator $\sum_a \zeta_a(l_a \cdot s_a)$ the summation extending over the six ligands supplying parameters ζ_X and ζ_Y for a MX_nY_{6-n} complex. Spin−orbitals are chosen to transform according to columns of irreducible representations of double groups. The correct linear combinations for $t_1 \times e' = e' + u'$ and $t_2 \times e' = e'' + u'$ combinations in O_h* are obtained from the tables of Griffith.[19] Transformation properties and orbital phases of ligand orbitals must be consistent for all spinorbitals of correct symmetry. For low-symmetry field calculations the orbital parts in the spin−orbitals are chosen identical to symmetry adapted molecular orbitals as used for spatial orbital interactions.

3.3. Calculations. The calculation on mixed ligand complexes MX_nY_{6-n} of symmetry C_{4v} (monosubstituted complexes), D_{4h} (trans-disubstituted), and C_{2v} (cis-disubstituted) is based on the octahedral orbital scheme and considers the energy level shifts and splittings due to ligand substitution using appropriate symmetry orbitals. In all cases orthoaxial metal−ligand geometry is assumed for simplicity. However, the AOM allows one to include real X−M−Y valence angles if necessary. The orbital basis is limited to ligand p orbitals which are in π bonding position relative to the metal which in the following is briefly noted as π MOs.

The results are compiled in Tables 1−4 where the orbital interaction and the spin−orbit perturbation matrixes are listed which are used in the following for interpreting the charge-transfer spectra of the present compounds. The spin−orbit energy matrices for $\zeta_X = \zeta_Y$ agree with earlier results reported for O_h* symmetry.[20]

(17) Collingwood, J. C.; Piepho, S. B.; Schwartz, R. W.; Dobosh, P. A.; Dickinson, J. R.; Schatz, P. N. *Mol. Phys.* **1975**, *29*, 793.
(18) Verdonck, E.; Vanquickenborne, L. G. *Inorg. Chim. Acta* **1977**, *23*, 67.
(19) Griffith, J. S. *The Theory of Transition-Metal Ions*; Cambridge University Press: Cambridge, U.K., 1961; p 400.
(20) Bird, B. D.; Day, P.; Grant, E. A. *J. Chem. Soc. (A)* **1970**, 100.

Table 1. Orbital Interaction Energies and Energy Matrix for Ligand π Molecular Orbitals of MX_5Y (C_{4v}); Notations as Given in the Theoretical Section

$$E(a_2) = -\sigma - \pi \text{ from } t_{1g}(O_h) \qquad E(a_1) = 2\pi \text{ from } t_{1u}$$

$$E(b_1) = -2\pi \text{ from } t_{2u} \qquad E(b_2) = \sigma + \pi \text{ from } t_{2g}$$

	e matrix			
	t_{1g}	t_{1u}	t_{2u}	t_{2g}
t_{1g}	$^1/_4\Delta E - {}^1/_2(\sigma + \sigma' + \pi + \pi')$	$-^1/_4(\Delta E + \Delta\sigma - \Delta\pi)$	$-^1/_4(\Delta E + \Delta\sigma + 3\Delta\pi)$	$-^1/_4\Delta E$
t_{1u}		$^1/_4\Delta E + \pi + \pi'$	$-^1/_4\Delta E$	$-^1/_4(\Delta E - \Delta\sigma - 3\Delta\pi)$
t_{2u}			$^1/_4\Delta E - \pi - \pi'$	$-^1/_4(\Delta E - \Delta\sigma + \Delta\pi)$
t_{2g}				$^1/_4\Delta E + {}^1/_2(\sigma + \sigma' + \pi + \pi')$

Table 2. Orbital Interactions for Ligand π MOs of *trans*-MX_4Y_2 (D_{4h}); $E(a_{2g})$, $E(a_{2u})$, $E(b_{2u})$, $E(b_{2g})$ Equal to Corresponding Energies as in C_{4v} (Table 1)

	e_g matrix			e_u matrix	
	t_{1g}	t_{2g}		t_{1u}	t_{2u}
t_{1g}	$^1/_2\Delta E - \sigma' - \pi'$	$^1/_2\Delta E$	t_{1u}	$^1/_2\Delta E + 2\pi'$	$^1/_2\Delta E$
t_{2g}		$^1/_2\Delta E + \sigma' + \pi'$	t_{2u}		$^1/_2\Delta E - 2\pi'$

4. Discussion

The assignment is based on the spectra of octahedral complexes OsX_6 (X = Cl, Br) and outlines band shifts and band splittings due to substitution of one or two of the ligands. Figure 1 illustrates the spectra of complexes with a majority of chloride ligands in comparison with the well-known $OsCl_6$ spectrum. In Figure 3 mixed ligand complexes containing more bromide ligands are compared with $OsBr_6$. The trans di-substituted complex plotted in Figure 2 will be discussed separately. The charge-transfer spectrum of the hexachloro Os(IV) complex has been assigned on the basis of MCD results to electron transitions from t_{1g}, t_{1u}, and t_{2u} ligand molecular orbitals into t_{2g} orbitals resulting from metal d orbitals.[3,5,6] Due to the large number of model parameters which is in excess to the number of peak positions to be identified, a fitting of theoretical parameter values to the experiment is not possible. However, relative sizes of parameters can be used for an interpretation of the spectra.

4.1. Chloro Complex Derivatives. $Cs_2[OsCl_5Br]$. All bands of the monosubstituted complex are shifted to smaller wavenumbers compared to the hexachloro spectrum: they are split due to symmetry reduction (cf. Figure 1).The shift toward lower energy for ligand to metal charge transfer corresponds to the decrease of ionization energy or optical electronegativity of Br compared to Cl.[21] The calculated ligand orbitals in π positions to the central metal (Table 1) for one-dimensional components a_1, a_2, b_1, and b_2 have, however, orbital energies that are identical to those for $OsCl_6$ orbitals, cf. eq 1. Only e components are predicted to shift, e.g., the e resulting from $t_{1g}(O_h)$ by $^1/_4(\Delta E) - {}^1/_2(\Delta\sigma + \Delta\pi) > 0$, i.e., the e orbitals will be higher in energy than a_2. Also this orbital sequence e > a_2 from t_{1g} will be unchanged when the nondiagonal elements between e levels are considered since estimation from second-order perturbation

$$e(t_{1g}) = \langle t_{1g}|H|t_{1g}\rangle + \sum_{\gamma \neq t_{1g}} \frac{|\langle t_{1g}|H|\gamma\rangle|^2}{\langle t_{1g}|H|t_{1g}\rangle - \langle \gamma|H|\gamma\rangle} \qquad (2)$$

pushes the e component further to higher energy while a_2 does not combine with any orbital within the set considered. The matrix elements of eq 2 are those of Table 1, the sum extending over $\gamma = t_{1u}, t_{2u}, t_{2g}$.

The long-wavelength shift also observed for one-dimensional C_{4v} levels which result from t_{1u} and t_{2u} is explained by combinations with lower lying σ MOs showing the importance of nondiagonal elements between different parent levels: i.e., when the symmetry is reduced from O_h to C_{4v} the lower σ MOs split into $e_g \rightarrow a_1 + b_1$, $t_{1u}\sigma \rightarrow a_1 + e$, and $a_{1g} \rightarrow a_1$. Although σ orbitals are much lower in energy than π, they can shift the a_1 component of $t_{1u}\pi$ (cf. Figure 5) by interaction with a_1 MOs resulting from e_g, $t_{1u}\sigma$, and a_{1g} and the b_1 component of t_{2u} by interaction with b_1 from e_g σ orbitals. Since a_2 occurs only from t_{1g}, it cannot be shifted by this mechanism. With this we obtain the orbital assignments given for the Cs_2 [$OsCl_5Br$] spectrum of Figure 1. An uncertainty arises on the assignment of t_{2u} components. The level sequence e > b_1 derived from the diagonal elements e - $b_1 = {}^1/_4(\Delta E) + \Delta\pi > 0$ could be reversed if stabilization due to e of t_{2u} by combination to e components of t_{1g} and t_{1u} is larger than destabilization due to e of t_{2g} and of $t_{1u}\sigma$ from lower energy. Since the absolute value of the nondiagonal element $\langle t_{2u}|H|t_{2g}\rangle$ entering in second order is larger than that of $\langle t_{2u}|H|t_{1u}\rangle$ (cf. Table 1) and t_{2g} and t_{1u} are the closest in energy to t_{2u}, we believe that the assumed orbital sequence e > b_1 is correct.

Selection rules from symmetry consideration (cf. Figure 5) evaluated for a system of four d electrons with $e^3b_2^1$ configuration in C_{4v} supply charge-transfer transitions from the ^3E ground state which are all allowed by electric dipole radiation; from the higher level $^3A_2$ of $^3T_{1g}(O_h)$ four out of seven transitions are allowed. This explains the intensities of the $OsCl_5$-Br bands, the lack of an inversion center gives rise to higher intensities also for the low-energy transitions which in O_h result from parity-forbidden transitions.

Parameter Relations. Due to the large number of parameters a conventional fit to the spectra cannot be carried out: in O_h we have σ and π parameters for interligand orbital interaction and another for $t_{1u}\pi - t_{1u}\sigma$ ligand orbital combination. For metal−ligand π bonding we must include parameters for p_π(metal)−t_{1u} and d_π(metal)−t_{2g} interaction for correct location of t_{1u} and t_{2g} in the ligand orbital scheme. For metal−ligand σ bonds additional parameters are necessary, and at lower symmetry ΔE, σ', and π' etc. parameters have to be added.

However, some relations between these parameters can be obtained from the observed orbital transitions. They may be, for instance, calculated in O_h from t_{1g} and t_{2u} ligand MOs which cannot combine through metal−ligand interactions. For a basis set of MX_6 containing ligand valence orbitals and d, s, and p on the central metal and s and p on the ligands, the resulting symmetry orbitals t_{1g} and t_{2u} do not combine by symmetry

(21) Jørgensen, C. K. *Orbitals in Atoms and Molecules*; Academic Press: London, 1969.

Table 3. Orbital Interactions for Ligand π MOs t_{1g}, t_{1u}, and t_{2u} of *cis*-MX_4Y_2 (C_{2v})

		a_1 matrix	
		t_{1u}	t_{2u}
	t_{1u}	$^1/_4\Delta E + {}^1/_8(\sigma - 2\sigma' + \sigma'' + 9\pi + 6\pi' + \pi'')$	$^1/_4\Delta E + {}^1/_8(-2\Delta\sigma + \Delta'\sigma - 2\Delta\pi + \Delta'\pi)$
	t_{2u}		$^1/_4\Delta E + {}^1/_8(\sigma - 2\sigma' + \sigma'' - 7\pi - 10\pi' + \pi'')$

	a_2 matrix		b_2 matrix		
	t_{1g}	t_{2u}		t_{1g}	t_{1u}
t_{1g}	$^1/_4\Delta E - {}^1/_4(2\sigma + 2\sigma' + 3\pi + \pi'')$	$(\sqrt{1/8})\Delta E + (\sqrt{1/8})(\Delta\sigma + \Delta\pi + \Delta'\pi)$	t_{1g}	$^1/_4\Delta E - {}^1/_4(2\sigma + 2\sigma' + \pi + 4\pi' - \pi'')$	$(\sqrt{1/8})\Delta E + (\sqrt{1/8})(\Delta\sigma + \Delta\pi - \Delta'\pi)$
t_{2u}		$^1/_2\Delta E - {}^1/_2(\pi + 2\pi' + \pi'')$	t_{1u}		$^1/_2\Delta E + {}^1/_2(\pi + 2\pi' + \pi'')$

	b_1 matrix		
	t_{1g}	t_{1u}	t_{2u}
t_{1g}	$^1/_2\Delta E - {}^1/_4(\sigma + 2\sigma' + \sigma'' + \pi + 2\pi' + \pi'')$	$(\sqrt{1/8})\Delta E + {}^1/_4(\sqrt{1/2})(-\Delta'\sigma + 4\Delta\pi - \Delta'\pi)$	$(\sqrt{1/8})\Delta E + {}^1/_4(\sqrt{1/2})(\Delta'\sigma - 4\Delta\pi + \Delta'\pi)$
t_{1u}		$^1/_4\Delta E + {}^1/_8(-\sigma + 2\sigma' - \sigma'' + 7\pi + 10\pi' - \pi'')$	$^1/_4\Delta E + {}^1/_8(2\Delta\sigma - \Delta'\sigma + 2\Delta\pi - \Delta'\pi)$
t_{2u}			$^1/_4\Delta E + {}^1/_8(-\sigma + 2\sigma' - \sigma'' - 9\pi - 6\pi' - \pi'')$

Table 4. Spin−Orbit Coupling Matrix for Ligand π MOs of MX_5Y (C_{4v}) with $\Delta\zeta = \zeta_X - \zeta_Y$

e′ matrix

O_h		t_{1g}		t_{1u}		t_{2u}	t_{2g}
	O_h^*	e'_g	u'_g	e'_u	u'_u	u'_u	u'_g
	e'_g	$-^1/_{12}(5\zeta_X + \zeta_Y)$	$-(\sqrt{2}/24)\Delta\zeta$	$^i/_{12}\Delta\zeta$	$-(\sqrt{2}/24)i\Delta\zeta$	$(\sqrt{2/3})^i/_8\Delta\zeta$	$-(\sqrt{2/3})^1/_8\Delta\zeta$
t_{1g}							
	u'_g		$^1/_{24}(7\zeta_X - \zeta_Y)$	$-(\sqrt{2}/24)i\Delta\zeta$	$^i/_{24}\Delta\zeta$	$-(\sqrt{1/3})^i/_8\Delta\zeta$	$-(\sqrt{1/3})^1/_8(5\zeta_X + \zeta_Y)^a$
	e'_u			$-^1/_{12}(5\zeta_X + \zeta_Y)$	$-(\sqrt{2}/24)\Delta\zeta$	$(\sqrt{2/3})^1/_8\Delta\zeta$	$(\sqrt{1/6})^i/_4\Delta\zeta$
t_{1u}							
	u'_u				$^1/_{24}(7\zeta_X - \zeta_Y)$	$(\sqrt{1/3})^1/_8(5\zeta_X + \zeta_Y)^a$	$-(\sqrt{1/3})^i/_8\Delta\zeta$
t_{2u}	u'_u					$-^1/_8(\zeta_X + \zeta_Y)$	$^i/_8\Delta\zeta$
t_{2g}	u'_g						$-^1/_8(\zeta_X + \zeta_Y)$

e″ matrix

O_h		t_{1g}	t_{1u}	t_{2u}		t_{2g}	
	O_h^*	u'_g	u'_u	e''_u	u'_u	e''_g	u'_g
t_{1g}	u'_g	$^1/_8(\zeta_X + \zeta_Y)$	$-^i/_8\Delta\zeta$	$(\sqrt{2/3})^i/_8\Delta\zeta$	$-(\sqrt{1/3})^i/_8\Delta\zeta$	$-(\sqrt{2/3})^1/_8\Delta\zeta$	$-(\sqrt{1/3})^1/_8(5\zeta_X + \zeta_Y)^a$
t_{1u}	u'_u		$^1/_8(\zeta_X + \zeta_Y)$	$(\sqrt{2/3})^1/_8\Delta\zeta$	$(\sqrt{1/3})^1/_8(5\zeta_X + \zeta_Y)^a$	$(\sqrt{1/6})^i/_4\Delta\zeta$	$-(\sqrt{1/3})^i/_8\Delta\zeta$
	e''_u			$^1/_{12}(5\zeta_X + \zeta_Y)$	$(\sqrt{2}/24)\Delta\zeta$	$^i/_{12}\Delta\zeta$	$(\sqrt{2}/24)i\Delta\zeta$
t_{2u}							
	u'_u				$-^1/_{24}(7\zeta_X - \zeta_Y)$	$(\sqrt{2}/24)i\Delta\zeta$	$-^i/_{24}\Delta\zeta$
	e''_g					$^1/_{12}(5\zeta_X + \zeta_Y)$	$-(\sqrt{2}/24)\Delta\zeta$
t_{2g}							
	u'_g						$-^1/_{24}(7\zeta_X - \zeta_Y)$

[a] The dominant part results from u′ symmetry functions of O_h^* combining t_1 and t_2. The low-symmetry contribution is $\pm(\sqrt{1/3})^1/_8(\Delta\zeta)$ for u'_g and u'_u, respectively.

reasons. The difference in orbital energies of eq 1 due to ligand−ligand interaction, i.e., $t_{1g} - t_{2u} = -\sigma + \pi$, then can be related to corresponding band peaks of the absorption spectrum of Figure 1 ($21\,600 - 29\,600 = -8000$ cm^{-1}). The observed metal−ligand charge-transfer bands therefore suggest a parameter relation of eq 3.

$$\sigma - \pi = -8000\ \text{cm}^{-1} \tag{3}$$

Since both σ and π are by definition negative, we expect a relatively large interligand σ-interaction, i.e., $|\sigma| > 8000$ cm^{-1} and as usual $|\pi| < |\sigma|$.

An estimation of low-symmetry parameters can be obtained from the low-energy peaks of $OsCl_5Br$ and $OsCl_6$ spectra assuming parameter transferability from one compound to the other. The shift $21\,060 - 21\,600 = 540$ cm^{-1} resulting from t_{1g} corresponds to the theoretical orbital difference of Table 1,

$$^1/_4\Delta E + {}^1/_2(\Delta\sigma + \Delta\pi) + e^{(2)} = 540\ \text{cm}{-}1 \tag{4}$$

where $e^{(2)} > 0$ is the shift of the e component of t_{1g} due to second-order terms resulting from nondiagonal elements to lower lying orbitals $e(t_{1u})$, $e(t_{2u})$, etc. The parameter ΔE is related to the t_{2u} band peaks of $OsCl_6$ ($29\,600$ cm^{-1}) and $OsBr_6$ ($23\,600$ cm^{-1} as estimated from taking the center of gravity, i.e., 1:2, due to spin−orbit component degeneracies) by eq 5.

$$\Delta E + 2\Delta'\pi = 6000\ \text{cm}^{-1} \tag{5}$$

This compares with optical electronegativities 3.0 of Cl and 2.8 of Br which refer to the highest bond orbitals of ligands.[21] With

the approximation $\Delta'\pi = 2\,\Delta\pi$ we have from eqs 4 and 5

$$\Delta\sigma - \Delta\pi \leq -1920\ \text{cm}^{-1} \text{ for } e^{(2)} > 0 \text{ or } = 0, \text{ respectively} \quad (6)$$

The difference of orbital electronegativities converted into wavenumbers yielding 6000 cm^{-1} suggests, however, that $\Delta\sigma$ and $\Delta\pi$ parameter relations derived from the preceding equations may be overestimated in their sizes.

Since bond changes, eq 6, differ less than bonding parameters, eq 3, and are as expected to be smaller (absolutely), consideration of nondiagonal energy matrix elements as perturbations of diagonal expressions as in eq 2 is justified.

$Cs_2[OsCl_4Br_2]$ (cis). In the spectrum of the disubstituted complex (Figure 1) we notice a further shift toward lower energy due to substitution of a second ligand and a somewhat larger band splitting. All bands are more intense due to the definite loss of the symmetry inversion center, as becomes evident from bands b_1, b_2, and a_2 resulting from $t_{1g}(O_h)$ which obtain similar intensity as those from t_{1u} and t_{2u}. The small absorption below 17 000 cm^{-1} is assigned to a ligand field transition into $\Gamma_1(^1A_{1g})$.[14]

Although all transitions t_{1g}, t_{1u}, and t_{2u} in O_h should be split in C_{2v} into three components by group theory, we only observe two band components in every case. This is well explained by the energies calculated from symmetry-adapted molecular orbitals listed in Table 3. Due to the large number of possible combinations, the calculations are limited to the t_{1g}, t_{1u}, t_{2u} π orbitals. If parameters are assumed to be related by mean values

$$\sigma' = {}^1/_2(\sigma + \sigma'') \text{ and } \pi' = {}^1/_2(\pi + \pi'') \quad (7)$$

which approximate Cl−Br interaction by Cl−Cl and Br−Br, the diagonal elements supply the following accidental degeneracies:

$$a_2(t_{1g}) = b_2(t_{1g}),\ a_1(t_{1u}) = b_1(t_{1u}), \text{ and } a_1(t_{2u}) = b_1(t_{2u}) \quad (8)$$

Equation 8 suggests an orbital assignment as indicated in Figure 1. The b_1 component of t_{1g}, b_2 of t_{1u}, and a_2 of t_{2u} exhibit larger shifts toward lower wavenumbers than their respective components. The nondiagonal elements remove the degeneracy only marginally since energy changes due to second-order terms are small: the a_2 and b_2 components of t_{1g}, for instance, are moved by similar amounts due to nondiagonal elements with $a_2(t_{2u})$ and $b_2(t_{1u})$ (Table 3) which differ only by $\sqrt{{}^1/_2}(\Delta'\pi)$ (although the energy denominators $t_{1g}-t_{2u}$ and $t_{1g}-t_{1u}$ in eq 2 differ as well). A closer analysis of second-order effects supplies energy shifts for quasidegenerate orbitals differing by about 500 cm^{-1}, which is well within the uncertainties resulting from band half-widths of 1000 cm^{-1} measured for these bands. Obviously, band resolution is too low to show a removal of accidental degeneracy. The calculated results further suggest a small energy shift ${}^1/_4(\Delta E) + {}^1/_2(\Delta\sigma) + {}^1/_4(\Delta'\pi)$ for a_2 and b_2 relative to the parent t_{1g} band of Cs_2OsCl_6. Depending on the size of $\Delta E > 0$ and $\Delta\sigma,\Delta\pi < 0$, this corresponds to a low- or high-energy shift. Parameter estimation from eqs 5 and 7 suggests a small low-frequency shift which is, however, not observed. The corresponding peak in Figure 1 is almost at equal energy which also cannot be explained due to changes of the ligand field energies on the metal d orbital side. We attribute this discrepancy to an increase of d orbital energies due to the lower effective charge on Os(IV) resulting from enhanced covalency of metal−ligand bonds on higher substitution of chloride by bromide (larger central field covalency[21]). This contribution leads to a moderate general blue shift of all charge-transfer bands in addition to all changes occurring from ligand−ligand orbital interactions so far mentioned.

$Cs_2[OsCl_4Br_2]$ (trans). The assignment of this spectrum plotted in Figure 2 is straightforward in view of the preceding results. Due to the conservation of the inversion center we can distinguish between Laporte-forbidden (low-intensity bands) and allowed (high intensity) transitions. The high symmetry (D_{4h}) limits the number of possible combinations. The peaks which are slightly shifted compared to the hexachloro complex are assigned to one-dimensional orbital levels in D_{4h} which is suggested by the interligand orbital energies of Table 2 and from intensity arguments as well (not all the transitions into d orbitals are allowed). The dimensions of the e_g and e_u matrixes are smaller; however, nondiagonal elements are rather large, leading to remarkable shifts. Indeed we see both e_u components in Figure 2 shifted toward lower energy, the shift of e_u from t_{1u} being much larger. This is rationalized from the e_u matrix of Table 2: the diagonal elements increase $e_u(t_{1u})$ relative to t_{1u} of O_h by ${}^1/_2(\Delta E) - 2\Delta\pi$ and $e_u(t_{2u})$ becomes somewhat smaller by ${}^1/_2(\Delta E) + 2\Delta\pi$, while the nondiagonal element pushes the $e_u(t_{1u})$ level further to higher energy and stabilizes $e_u(t_{2u})$. This explains the highly unsymmetrical e_u -band shifts compared to the octahedral bands leading to shifts toward lower wavenumbers, pushing $e_u(t_{1u})$ by 2810 cm^{-1} and $e_u(t_{2u})$ by 1600 cm^{-1}. Closer numerical analysis would require reliable values for the model parameters involved. Since interactions with lower lying M−L σ orbitals are expected to be large as well, the actual parameter sizes cannot be estimated due to the lack of information on these level energies. They will, however, not interfer with the assignment carried out on the basis of M−L π orbitals.

It should be noted that the present assignment agrees with that of Jørgensen and Preetz[5] but is different for t_{2u} to the work of Schatz et al.[7] from which a $b_{2u} < e_u$ low-symmetry band sequence has been derived. However, the latter spectrum has large vibrational fine structure and is recorded from samples contaminated with the cis isomer.[22]

4.2. Bromo Complex Derivatives. A_2OsBr_6. The charge-transfer spectrum of the hexabromo complex is well interpreted.[1,4,5,20] The assignment takes the spin−orbit coupling on the bromo ligands into account which is much larger than that of chloro ligands, e. g., in the free atom the spin−orbit coupling parameter is 590 cm^{-1} for Cl and 2460 cm^{-1} for Br. Band splittings due to this coupling can be detected already in the solution spectrum.[1] Moreover, spectra of Os^{4+} doped in Cs_2ZrBr_6 crystals exhibit extensive vibrational fine structure which in part could be assigned to normal vibrations due to the complex octahedron.[4] Our spectrum recorded from pure Cs_2OsBr_6 (Figure 3) exhibits only the main contours of doped material spectra and is somewhat shifted to lower wavenumbers. Assignments to spin−orbit level components as indicated in the figure agree with earlier results and are consistent with energy matrix elements obtained from MX_5Y of Table 4 when Y equals X. In particular, we assign the small 19 880 cm^{-1} band to the $e'_u(O_h^*)$ component of $t_{1u}(O_h)$, which in strict octahedral environment is symmetry forbidden (Figure 5) but may become allowed by vibronic coupling. This transition has been identified in MCD of $Cs_2ZrBr_6:Os^{4+}$ as vibrational sidebands which in

(22) Barka, G.; Preetz, W. *Z. Anorg. Allg. Chem.* **1977**, *433*, 147.

absorption appear as shoulders imposed on the broad e''_u band of the strong charge-transfer transition resulting from t_{2u}.[4] The large splitting of the first charge-transfer band t_{1u} into u'_u and e'_u compared to the others results from a combined second-order effect due to u'_u combinations of $t_{1u}\pi$ and $t_{2u}\pi$ ligand orbitals[3] and of $t_{1u}\pi$ and $t_{2u}\pi$, the latter providing the matrix elements $\pm(\sqrt{3}/4)\zeta_{Br}$ in Table 4 (for $\zeta_X = \zeta_Y$ in O_h* symmetry). Since there are no other electronic transitions in octahedral symmetry, we must attribute the 18 810 cm^{-1} band and the weak shoulder on the high-energy flank of the 17 360 cm^{-1} peak to superpositions of various vibronic transitions which are not as well resolved as in the spectra of doped materials.[4,20]

We notice, however, a large dependence of the complex spectrum on the counterion: Figure 4 compares, e.g., the 2 K charge-transfer absorption spectra of potassium and tetrabutylammonium salts recorded using the same experimental conditions. A remarkable shift toward higher wavenumbers in the series of K, Cs, and Bu_4N salts is evident (s. Figure 3 for Cs) which has been explained by larger Os−Br atomic distances due to increased unit cells for bulky cations.[1] This is supported by the bathochromic shift of the K_2OsBr_6 spectrum when applying external pressure.[23] The Bu_4N complex spectrum is different in some other aspects due to the lower symmetry of the OsX_6 chromophore which is also noticed in the ligand field spectrum.[14] The low $e'_u \rightarrow e''_g$ band at 19 880 cm^{-1}, forbidden in O_h*, moves to 21 880 cm^{-1} and is much more intense. The other component, $u'_u \rightarrow e''_g$, around 19 400 cm^{-1} now exhibits vibrational fine structure, the profile being strongly temperature dependent. The small absorptions at lower frequency are due to the first spin−orbit component of t_{1g} which in alkali salt spectra is covered by transitions from t_{1u}. Some essentials of the Bu_4N spectrum are very similar to those reported for the ethylammonium salt[20]; in either case the intensity of the 21 880 cm^{-1} peak is very high, and there is a large temperature dependence in the 19 400 cm^{-1} region, the reason for which remaining obscure.

$Cs_2[OsBr_5Cl]$. The spectrum of the chloro-substituted complex is shifted to higher energy with respect to Cs_2OsBr_6 (cf. Figure 3) which corresponds to the similar low energy shift in compounds with reverse ligand composition as outlined in the previous section. Due to larger spin−orbit splittings, the spectra of bromo complex derivatives have more bands and assignments will be more elaborate. A total of nine electronic transitions is predicted from t_{1g}, t_{1u}, and t_{2u} by symmetry reduction to C_{4v}* (double group). In the spectrum of $Cs_2[OsBr_5Cl]$ (Figure 3) we can identify only five maxima and some shoulders and inflections. Transitions resulting from t_{1g} presumably have lower intensities than others (similar to what was observed for $OsCl_5Br$) and are largely covered by stronger bands resulting from $e'(u'_u)$, $e''(u'_u)$, $e'(e'_u)$ of t_{1u} as obtained for Cs_2OsBr_6 (cf. Figure 5). The orbital interaction matrix for $OsBr_5Cl$ is listed in Table 1; that for spin−orbit coupling is listed in Table 4. The parameter relations in this case are $\Delta E < 0$, $\sigma > \sigma'$, $\pi > \pi'$, and $\zeta_X > \zeta_Y$.

As previously the energy splittings of octahedral spin−orbit levels of $OsBr_6$ due to lower symmetry will be discussed (cf. Figure 5). Restriction to diagonal matrix elements supplies the following orbital energy changes relative to t_{1u} of $OsBr_6$ on substitution of one Br by Cl (cf. Tables 1 and 4).

$$C^*_{4v}: \quad \begin{aligned} e'(a_1) &= \frac{1}{12}\Delta\zeta && \text{from } e'_u(O_h^*) \\ e'(e) &= \frac{1}{24}\Delta\zeta + \frac{1}{4}\Delta E - \Delta\pi' \\ e''(e) &= -\frac{1}{8}\Delta\zeta + \frac{1}{4}\Delta E - \Delta\pi' \end{aligned} \Bigg\} \text{ from } u'_u(O_h^*) \qquad (9)$$

The parameter relations supply an orbital sequence of increasing energy as

$$e'(a_1) < e''(e) < e'(e) \qquad \text{from } t_{1u} \qquad (10)$$

The intensity arguments favoring even-to-odd transitions predict $e'(e)$ from t_{1u} assignment to the absorption peak of lowest energy (18 010 cm^{-1}). Inclusion of nondiagonal elements will not change this assignment due to repulsion to all other e' levels of lower energy. According to eq 9 the $e'(a_1)$ component should move to higher energy ($\Delta\zeta > 0$), the corresponding transition therefore is predicted to shift to lower frequency which for the assignment given is not the case: the corresponding band changes from 19 880 cm^{-1} for $OsBr_6$ to 20 770 cm^{-1} (e') for $OsBr_5Cl$ (Figure 3). Since this shift cannot be reversed by inclusion of central field covalency increasing the effective charge on Os on substitution of Br by Cl, it must be due to nondiagonal elements by coupling higher energy e' wave functions to $e'(a_1)$, the largest contribution resulting from $\langle e'(e'_u)|H|e'(u'_u)\rangle = -(\sqrt{2}/24)(\Delta\zeta)$ in Table 4. Attributing the 20 770 cm^{-1} peak to $e''(b_1)$ arising from t_{2u}, which would mean a 1430 cm^{-1} shift to lower energy in contrast to all other bands, is less probable because diagonal elements of the t_{2u} sequential levels rather suggest a high-frequency shift.

The interaction with t_{1g} wave functions of lower symmetry, which combine with t_{1u} functions due to the removal of the inversion center, leads to larger changes. The orbital sequence (cf. Figure 5) inferred from diagonal elements is calculated as

$$e'(a_2) < e''(e) < e'(e) \qquad \text{from } t_{1g} \qquad (11)$$

We expect the two e' levels to move the $e'(t_{1u})$ toward lower energy (see $t_{1g}-t_{1u}$ nondiagonal elements in Table 4) which is most effective because orbitals resulting from t_{1g} and t_{1u} are the closest in energy. Since transitions from t_{1g} orbitals have lower intensities, we observe these absorption only in the broadening of the 18 010 cm^{-1} (e') and the low energy shoulder of the 19 720 cm^{-1} band (e'') in the t_{1u} absorption region (Figure 3). More evidence on these transitions is obtained from the $OsBr_4Cl_2$ (cis) spectrum.

The spectrum higher than 22 000 cm^{-1} is dominated by transitions arising from t_{2u} ligand orbitals. The sequence calculated from diagonal elements of Tables 1 and 4 is

$$e''(e) < e'(e) < e''(e) \qquad \text{from } t_{2u} \qquad (12)$$

which suggests the band assignment as given in Figure 3. Since levels above and below are more distant in the orbital energy diagram, the coupling to other e' and e'' wave functions should not interfere with the sequence of eq 12. In this case the highest orbital level $e''(b_1)$ changes by $-1/2(\Delta\zeta) < 0$ relative to e''_u-(O_h*) toward lower energy, predicting a high-frequency band shift as observed in the spectrum, i.e., from 22 200 cm^{-1} for $OsBr_6$ to 23 090 cm^{-1} for $OsBr_5Cl$.

$Cs_2[OsBr_4Cl_2]$ (cis). This spectrum (Figure 3) is shifted further to higher energy. Since the C_{2v}* double group has only one irreducible representation e', symmetry assignments are not

(23) Balchan, A. S.; Drickamer, H. G. *J. Chem. Phys.* **1961**, *35*, 356.

informative. Therefore a calculation of the spin−orbit matrix which is of high dimension was not carried out. Due to Kramers degeneracy, no further splitting than that obtained for $OsBr_5Cl$ (C_{4v}*) is possible. Affiliation of bands to octahedral parent levels can, however, be discussed. The bands higher than 23 000 cm^{-1} can be attributed to transitions resulting from t_{2u} and the stronger peaks, 18 750, 20 890, and 21 670 cm^{-1}, from t_{1u}. Intensity arguments as used for $OsBr_5Cl$ attribute the 18 100 and 20 020 cm^{-1} shoulders to t_{1g} which are more intense than their equivalents in the $OsBr_5Cl$ spectrum (Figure 3) because of the more efficient removal of the inversion center in the cis-disubstituted complex. Further evidence cannot be obtained from arguments based on qualitative considerations.

5. Conclusions

Ligand to metal charge-transfer spectra of low-symmetry transition group ion complexes can be interpreted applying semiempirical molecular orbital theory which takes inter-ligand interaction into account as an important contribution. As in octahedral complex compounds assignment of absorption bands to orbital transitions is possible in the j−j coupling limit. For the spectral band resolution obtained, the inclusion of spin−orbit coupling on the ligands is necessary only for heavy ligands (e.g., Br). Due to the number of model parameters which exceeds the number of transitions possibly observable, eigenvalue calculations from perturbation matrixes are not recommended. However, relative parameter values are in general sufficient for carrying out reliable assignments for most of the bands to electronic transitions and to levels split by lower symmetry. The calculated orbital patterns show a remarkable parallelism to those in ligand field theory: orbital series and energy degeneracies for C_{4v} and D_{4h} complexes follow in the same sense and corresponding sequences for C_{2v} complexes (including accidental degeneracies) are reversed in the energy diagram (cf. Figure 5). The method evidently works optimal for systems of high symmetry due to symmetry restrictions. Other well-resolved charge-transfer spectra of mixed ligand complexes should be investigated on the basis of the present model.

Acknowledgment. The authors are grateful to Degussa Company, Hanau, for supplying us with Os compounds and to the Deutsche Forschungsgemeinschaft, Bonn-Bad Godesberg, for financial support.

IC980168+